Eur Biophys J (1998) 27: 237–245

ARTICLE

Tanja Pott · Maïté Paternostre · Erick J. Dufourc

A comparative study of the action of melittin on sphingomyelin and phosphatidylcholine bilayers

Received: 12 May 1997 / Revised version: 22 December 1997 / Accepted: 15 January 1998

Abstract To investigate whether lipid solubilization is of relevance in describing the interaction between melittin and biological membranes, we studied melittin-induced polymorphism using model membranes composed of the biological lipid sphingomyelin (bovine brain). The behavior of the system was monitored by solid state ^{31}P-NMR and turbidity measurements and compared to the peptides well-characterized action on the synthetic lipid dipalmitoylphosphatidylcholine. It was found that melittin-induced macroscopic changes of sphingomyelin membranes are qualitatively the same as in the case of dipalmitoylphosphatidylcholine bilayers. The sphingomyelin/melittin system is thus proposed to show a reversible vesicle-to-disc transition (fluid-to-gel phase) through an intermediate fusion or aggregation event centered at the main transition temperature, T_m, as reported in the case of saturated phosphatidylcholine. In the case of spontaneous disc formation at 37 °C, the lipid-to-peptide molar ratio in the discoidal objects was determined to be approximately 20 for dipalmitoylphosphatidylcholine and about 12 in the case of natural sphingomyelin. Melittin partition coefficients between membranes and the aqueous medium at 37 °C were found to be 6.1±0.8 mM^{-1} and 3.7±0.4 mM^{-1} for sphingomyelin and dipalmitoylphosphatidylcholine, respectively. For very high peptide quantities (lipid-to-peptide molar ratio, $R_i \leq 5$) mixed micelles are formed over the entire temperature range (20° to 60 °C) for both kinds of lipids.

Key words Amphiphatic helix · Lipid bilayer · Sphingomyelin · Turbidity measurements · ^{31}P solid state NMR · Membrane fragmentation

T. Pott · E. J. Dufourc
Centre de Recherche Paul Pascal, CNRS, F-33600 Pessac, France

M. Paternostre (✉)
Physicochimie des Systèmes Polyphasés, CNRS URA 1218,
Tour B, Faculté du Pharmacie, 5 Rue J. B. Clément,
F-92296 Châtenay-Malabry, France

Introduction

Melittin, the toxic peptide of honeybee (apis mellifera) venom (50% of its dry weight) is a basic, amphipathic, 26 residue polypeptide and is one of the best characterized peptides in terms of its interactions with natural and artificial membranes. The peptide induces a large range of membrane-based phenomena (for a review, see (Hider et al. 1983; Dempsey 1990)), such as lysis of natural and artificial membranes (Sessa et al. 1969; Habermann 1972), enhancement of passive ion permeability (Habermann and Jentsch 1967; Olson et al. 1974), membrane fusion (Murata et al. 1987; Ohki et al. 1994), formation of voltage-dependent ion channels (Hanke et al. 1983; Tosteson and Tosteson 1984; Smith et al. 1994), activation of phospholipase A_2 (Mollay and Kreil 1974), concentration dependent activation or inhibition of adenylate cyclase (Lad and Shier 1980) and inhibition of calmodulin (Compte et al. 1983). The conformation and assembly of mellitin in solution or in its lipid-associated state have been investigated by a wide variety of techniques (Brown et al. 1982; Hermetter and Lakowicz 1986; Brauner et al. 1987; Frey and Tamm 1991; Weaver et al. 1992; Smith et al. 1994; Cornut et al. 1996; Flach et al. 1996). The effects of melittin on phospholipid dynamics and organization have also been extensively studied. In such systems mellitin is able to induce a surprising variety of morphologically different phases depending on the bilayer's lipid composition, i. e., an H_{II}-phase (Batenburg et al. 1987), a cubic phase (Colotto et al. 1991) and different isotropic phases (Dufourc et al. 1986 a, Dufourcq et al. 1986) have indeed been reported. Melittin-induced lipid solubilization has further been suggested to be directly related to its strong hemolytic action (50% hemolysis of human erythrocytes at a lipid-to-peptide molar ratio, R_i, of approximately 20) (Dufourc et al. 1989; Katsu et al. 1989). However, in a different study the absence of significant mellitin-triggered lipid solubilization was reported (Maulet et al. 1984). With the aim of achieving a better understanding of the interaction of mellitin with biological membranes, we have investi-

gated its action on natural sphingomyelin, SM, and compared it with the well-characterized DPPC/melittin system (Dufourc et al. 1986a, b; Dufourcq et al. 1986; Faucon et al. 1995). Although SM is one of the major lipid components of the erythrocyte and cellular membranes of mammals in general and is mainly located in the outer leaflet (for review, see (Barenholz and Thompson 1980)), this is the first systematic study of SM/melittin systems. In the context of melittin-induced hemolysis it is important insofar as SM constitutes, together with unsaturated phosphatidylcholines, the bulk of phospholipids in the red blood cell outer leaflet, with which the peptide will associate first. SM is a rather peculiar naturally occurring phospholipid as it exhibits a gel-to-fluid transition temperature in the physiological temperature range (around 40 °C (Shipley et al. 1974)), that has been proposed to be of importance in the context of biological membranes (Boggs 1987; Curatolo 1987).

Herein, we used solid state ^{31}P-NMR and turbidity measurements as a function of temperature and melittin concentration to follow the peptide-triggered polymorphic behavior of the systems. Both methods have proven to be powerful tools to monitor polymorphic behavior (Burnell et al. 1980; Seelig and Seelig 1980; Ollivon et al. 1988; Faucon et al. 1995). Turbidity measurements were performed to determine the peptide-to-lipid molar ratios in the small melittin-induced objects formed spontaneously at 37 °C and to have an estimation of the partition coefficient of melittin between the solution and the two types of artificial membranes used, i. e., DPPC and natural sphingomyelin.

Materials and methods

Sphingomyelin from bovine brain was purchased from Fluka (France), SM (1) and from Sigma (France), SM (2). Dipalmitoylphosphatidylcholine, DPPC, was obtained from Avanti Polar Lipids (USA). Highly purified melittin was obtained from Serva (France). For NMR measurements DPPC dispersions were prepared according to established procedures (Pott and Dufourc, 1995). Because SM dispersions have a tendency to spontaneously form small vesicles (budding (Döbereiner et al. 1993)), the method leading to the smallest percentages of small vesicles was applied for preparation of NMR samples. In brief, a dry lipid film (50 mg) was dispersed in 0.5 ml of the appropriate buffer, then heated to 50° – 60 °C and submitted to gentle agitation until a homogeneous dispersion was obtained. In the case of turbidity measurements small unilamellar vesicles were obtained by sonication as described in Lesieur et al. (1990). Vesicles were prepared at 10 mM total lipid in buffer, stored under nitrogen and diluted prior to experiments. A Tris buffer system (100 mM Tris, 100 mM NaCl, 2 mM EDTA, pH = 7.5) was used, this induces a tetrameric state for the toxin in solution (Faucon et al. 1979; Talbot et al. 1979; Bello et al. 1982; Podo et al. 1982). Appropriate amounts of melittin were solubilized in the same buffer, added to the lipid dispersion and, in the case of thermal variations, incubated for at least 30 min at high temperature. Thin layer chromatography has been performed before and after completion of experiments; samples were found to be free of degradation products.

^{31}P-NMR was carried out on a Bruker ARX300 equipped for high power solid state spectroscopy and operating at 121.49 MHz; a phase-cycled Hahn-echo pulse sequence (Rance and Byrd 1983) with gated proton decoupling and quadrature detection was used. Samples were allowed to equilibrate for at least 30 min at a given temperature before the NMR signal was acquired; the temperature was regulated to ±1 °C. Thermal variations were performed by decreasing the temperature. Typical acquisition parameters were: spectral window of 64 kHz; $\pi/2$ pulsewidth of 8 μs; interpulse delay of 40 μs; recycle delay of 6 s; number of scans: 1000 – 1500. Spectral "dePaking" was performed as described elsewhere (Bloom et al. 1981; Sternin et al. 1983) and calculated for bilayer normals oriented at 90° with respect to the magnetic field direction. The amount of isotropic line superimposed on a powder pattern was determined by simulation of a Gaussian or Lorentzian line and subsequent subtraction from the experimental spectrum (Pott and Dufourc 1995). Percentages are expressed relative to the total spectral area.

Turbidity measurements were performed at 450 nm on a Perkin Elmer Lambda 2 double beam spectrophotometer equipped with a temperature regulation system. Errors in the temperature regulation were estimated to be about ±1.5 °C for thermal variations and ±0.5 °C for measurements at constant temperature. A paddle cuvette stirrer and a thermocouple that do not interfere with the light path were placed into the quartz cuvette containing the lipid dispersion. In the case of thermal variations, samples were sealed. For continuous measurements of solubilization at 37 °C a melittin solution was slowly and continuously injected through a thin tube connected to a thermostatted precision glass syringe (Hamilton, Reno, NV), which was pushed by a syringe pump (EDCO Scientific, Chapel Hill, NC).

Results

Temperature dependence of the action of melittin

The effects of melittin on membrane macroscopic organization were investigated by solid state ^{31}P-NMR and turbidity measurements on lipid dispersions as a function of temperature and melittin concentration. It should be noted that, with SM as lipid compound, two different batches differing in T_m have been used. The batches used for NMR and turbidity experiments exhibit broad transitions centered at ≈37 °C for SM (1) and ≈43 °C for SM (2), respectively. Such a shift in T_m is a common phenomenon for natural lipids and is usually due to differences in the fatty acyl chain composition between different batches. Representative ^{31}P-spectra of the SM (1)/melittin systems are pre-

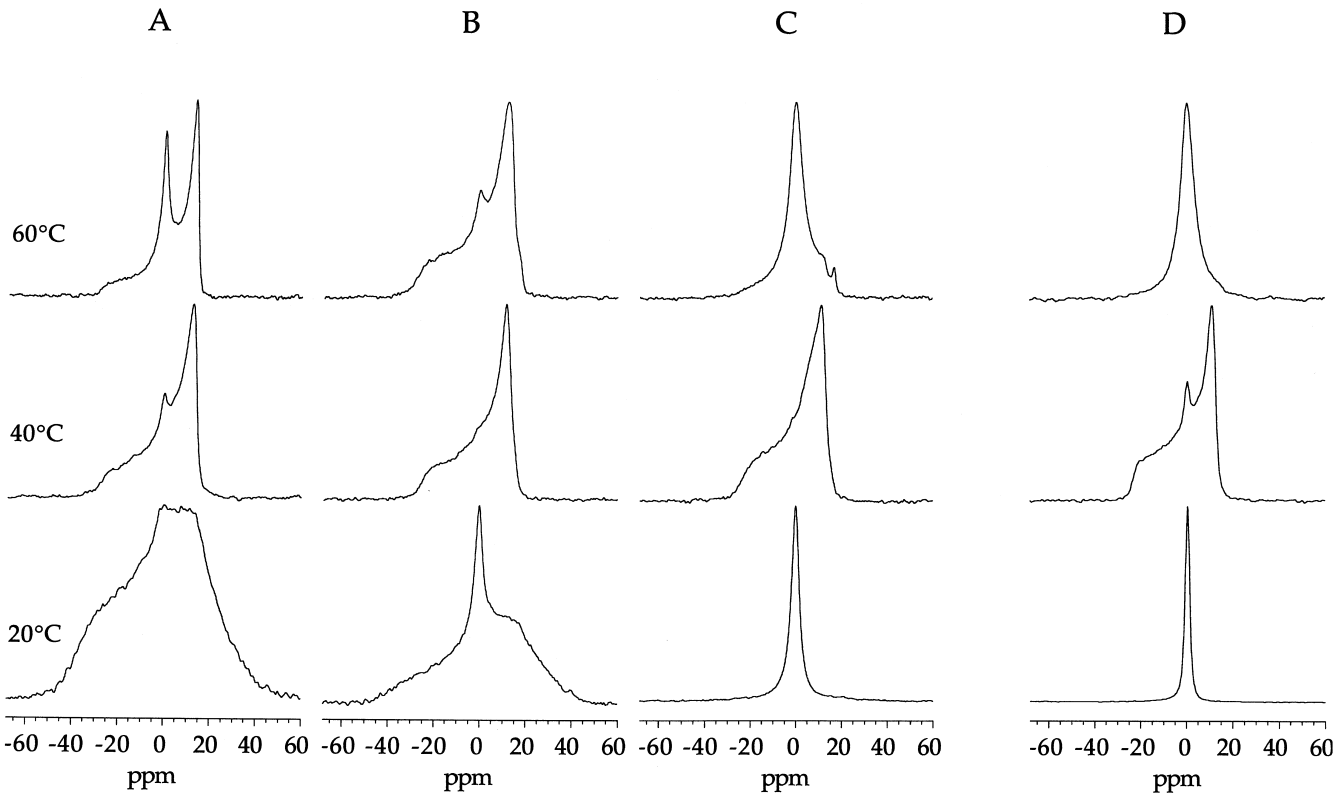

Fig. 1 Selected ^{31}P-NMR spectra of the SM (1)/melittin systems in the fluid phase, 60 °C, at approximately T_m, 40 °C, and in the gel phase, 20 °C, at (*A*) $R_i = \infty$, (*B*) $R_i = 50$ and (*C*) $R_i = 20$. For comparison, spectra of the DPPC/melittin system, $R_i = 20$, at the same temperatures are presented in (*D*). All thermal variations were performed by decreasing the temperature

sented in Fig. 1 A – C ($R_i = \infty$, 50 and 20); for comparison, data for the DPPC/melittin system are also shown (Fig. 1 D, $R_i = 20$). In contrast to pure DPPC bilayers, the SM membrane exhibits a strong tendency to vesiculate spontaneously (Döbereiner et al. 1993). In the ^{31}P-NMR measurements this is reflected by the presence of an isotropic line superposed on an axial symmetric powder pattern (Fig. 1 A). It can further be noted that the vesiculation process depends on the temperature and is more important in the fluid phase; similar behaviour was reported by Nezil and co-workers (Nezil et al., 1992). The addition of small amounts of melittin, $R_i = 100$, has negligible influence on this behavior (data not shown). A higher peptide amount, $R_i = 50$, leads to some modifications in the spectral shape (Fig. 1 B). In the fluid phase of sphingomyelin the amount of isotropic line is decreased. Contrastingly, in the gel phase one notes the appearance of an isotropic line superposed on the gel phase powder pattern. At $R_i = 20$ and in the fluid phase at 60 °C, a broad and slightly asymmetric isotropic line dominates the spectra of the SM (1) and DPPC systems (Fig. 1 C and D). Yet, a small difference between the two systems in the fluid phase can be noted. In the SM (1) system an anisotropic lipid fraction persists and gives rise to two further powder patterns, behavior that is not observed for DPPC, even at higher R_i. However, both peptide containing systems ($R_i = 20$) show a very similar evolution with temperature. At 40 °C one observes a powder pattern for both systems and a weak amount of isotropic line only in the case of DPPC. On decreasing the temperature into the lipid gel phase, both systems are characterized by a narrow isotropic line in the ^{31}P-NMR spectra.

To allow a more detailed analysis, the percentages of isotropic line in the SM (1) and DPPC systems were calculated by spectral simulation. The results for different peptide concentrations as a function of temperature are presented in Fig. 2. The general behavior of both lipid/peptide systems is quite similar. At $R_i = 20$ the toxin causes important amounts of isotropic line in the fluid and gel phase of both systems, but not in the transition region. Moreover, both kinds of lipid show a strong decrease in the isotropic linewidth at half height, $\Delta\nu_{1/2}$, when decreasing the temperature from the fluid into the gel phase (Table 1). For both peptide containing systems $\Delta\nu_{1/2}$ is around 250 Hz for $T < T_m$ and between 750 to 1100 Hz for $T > T_m$. However, some differences in the melittin-induced effects on SM and DPPC bilayers can nevertheless be noted. At $R_i = 20$, essentially all DPPC molecules show isotropic averaging on the NMR timescale whatever the temperature, except for $T \approx T_m$ (40 °C). Yet, at the same concentration the peptide does not produce a complete disappearance of the powder pattern in the case of SM (1) in the fluid phase. It can further be noted that the proximity of T_m (≈37 °C) leads already at 45 °C to a notable decrease in isotropic line in con-

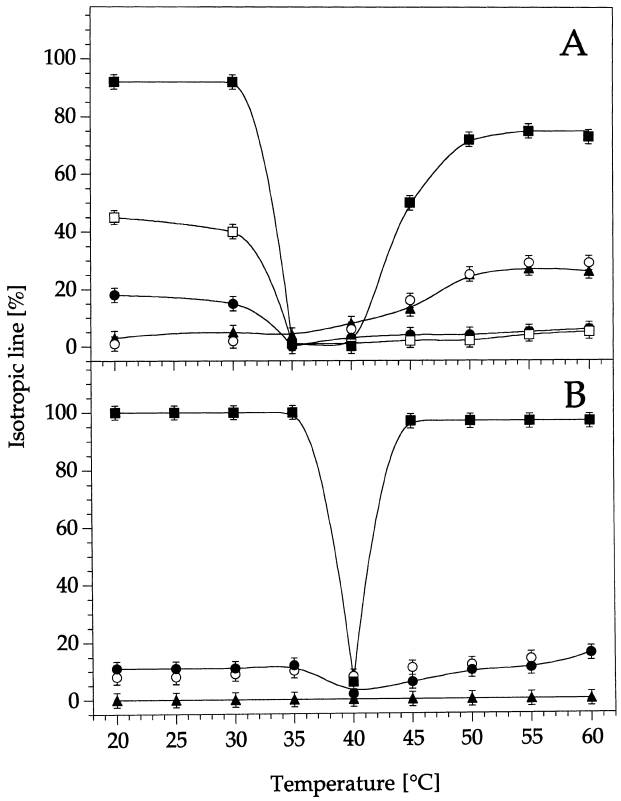

Fig. 2 A, B Percentages of isotropic line in the SM (1)/melittin (**A**) and the DPPC/melittin (**B**) systems as a function of temperature. $R_i = \infty$ (▲), $R_i = 100$ (○), $R_i = 50$ (●), $R_i = 30$ (□), $R_i = 20$ (■). Percentages are expressed relative to the total spectral area. Lines are drawn to help in reading the figure

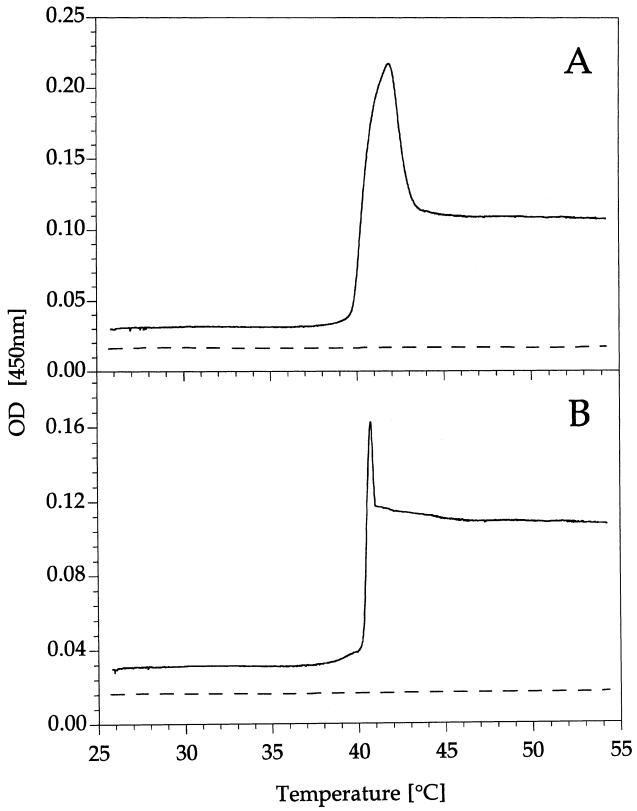

Fig. 3 A, B Variations of the optical density at 450 nm as a function of temperature for the SM (2)/melittin (**A**) and DPPC/melittin (**B**) systems at two different peptide concentrations: $R_i = 10$ (*solid line*) and $R_i = 5$ (*dashed line*). Lipid concentration was 1 mM. The thermal variation was carried out by a continuous decrease in temperature (0.18 °C/min) after incubation of the systems at 60 °C

Table 1 $\Delta\nu_{1/2}$ (in Hz) of the isotropic ^{31}P-NMR signal for both phospholipid/melittin systems at $R_i = 20$ and various temperatures

	20 °C	25 °C	30 °C	45 °C	50 °C	55 °C	60 °C
SM (1)	270	250	260	880	950	910	770
DPPC	240	230	240	900	1100	1020	750

Accuracy is ±10%

trast to the glycerolipid. Further, the temperature range where no isotropic line is detected is larger than for the DPPC, which indeed parallels the broad transition of natural SM when compared to DPPC. Also, in the gel phase of the SM (1) system, a smaller amount of anisotropically organized lipid appears to subsist in contrast to the DPPC system. The behavior of the two systems at low melittin content also seems to be different. At $R_i = 100$ the amount of isotropic line as well as its $\Delta\nu_{1/2}$ in the SM (1)-spectra correspond to the isotropic line observed for the peptide-free bilayer and almost no isotropic line is detected in the lipid's gel phase (see Fig. 2 A). This is somewhat in contrast to the DPPC system, where the toxin-induced amount of isotropic line is about the same for $R_i = 100$ and $R_i = 50$ (Fig. 2 B) and both gel and fluid phase spectra are affected by melittin.

To further characterize the influence of melittin on the two model membranes, turbidity measurements as a function of temperature were performed. Experiments on SM (2) ($T_m \approx 43$ °C) and DPPC SUV (phospholipid concentration 1.0 mM) were carried out by addition and incubation with the peptide at 60 °C followed by decreasing the temperature (0.18 °C/min.). To ensure that the chosen cooling rate had no influence on the kinetics of the systems, slower cooling rates, similar to those described in Faucon et al. (1995) were tested; no differences could be detected. During incubation at $R_i = 10$ (corresponding to a phospholipid-to-bound peptide molar ratio of 11 to 13, see discussion) and ≈60 °C and for both lipid systems the turbidity of the sample increases until it reaches a constant value approximately 15 min after the injection of melittin. The optical density, OD, then remains approximately constant for $T > T_m$ (OD≈0.11). When decreasing the temperature into the region of the T_m, an important increase in OD is detected, followed by a sudden drop down to very low OD at ≈40 °C (OD≈0.03, Fig. 3). The general thermal behavior of the SM (2) and the DPPC/peptide systems are very similar. The only difference between the two systems is the extent of the temperature region where strong turbidity changes occur, i. e., a larger one for the natural sphingolipid ($\Delta T \approx 4$ °C) than for the synthetic glycerolipid

($\Delta T \approx 1\,°C$). It should be noted that the sharp peak in turbidity at $T \approx T_m$ is extremely sensitive to the experimental conditions and the peptide concentration (data not shown). An increase in the melittin content results in a progressive decrease in the maximum OD for this peak. Moreover, stirring speed as well as cooling rate seem to affect this peak. For higher peptide concentration ($R_i = 5$) the OD of both lipid systems decreases during incubation down to ≈0.02 and then stays constant over the whole temperature range investigated (Fig. 3).

Effect of the phospholipid concentration on melittin-induced solubilization at 37 °C

Melittin-induced disc formation in DPPC bilayers has been reported to occur spontaneously and without high temperature incubation for $T_p < T < T_m$ (Monette et al. 1993; Pott and Dufourc 1995; Pott et al. 1996). This was verified herein by turbidity measurements. In this case melittin was added to the vesicles at 20 °C and the temperature was increased continuously (data not shown). For DPPC as well as for SM (2) vesicles the peptide induces a clearing of the samples between ≈35 °C and ≈39 °C. To characterize this solubilization process we followed the method employed earlier for detergent-induced vesicle-to-micelle transition (Ollivon et al. 1988; Paternostre et al. 1988). Since the critical peptide concentration to induce complete solubilization is dependent on the lipid concentration, turbidity measurements as a function of melittin concentration at a constant temperature of 37 °C were conducted for various phospolipid concentrations. Typical curves as a function of peptide concentration obtained with SM (2) and DPPC are shown in Figs. 4 A and B, respectively (initial lipid concentration: 0.4 mM). For both kinds of phospholipid the peptide first induces an increase in the OD. At a given toxin concentration the behavior of the systems changes and further injection of melittin results in a progressive decrease in OD until the solubilization process is complete and the OD remains almost constant. From this observation three main break points were defined and determined by the intercept of the tangents to the curves for both lipid/peptide systems according to Ollivon et al. (1988) and Paternostre et al. (1988) (see also Fig. 4). The first one, *a*, corresponds to the onset of the increase in OD, break point *b* is defined at the beginning of the OD decrease and for peptide concentrations higher than *c* solubilization is complete. Despite this resemblance in the general behavior of the two systems, it can be recognized that the peptide concentrations necessary to attain these break points are quite different. In the case of the DPPC system the OD starts to increase at very low toxin content, that is to say almost instantly (Fig. 4 B), whereas for the sphingolipid a higher peptide concentration has to be reached before a sharp increase in the OD is detected. A similar shift in the peptide content needed for complete solubilization is also detected (Fig. 4). In contrast, for the SM (2) system a maximum OD is reached at lower melittin concentration than for the DPPC system. To ensure that the morphological changes

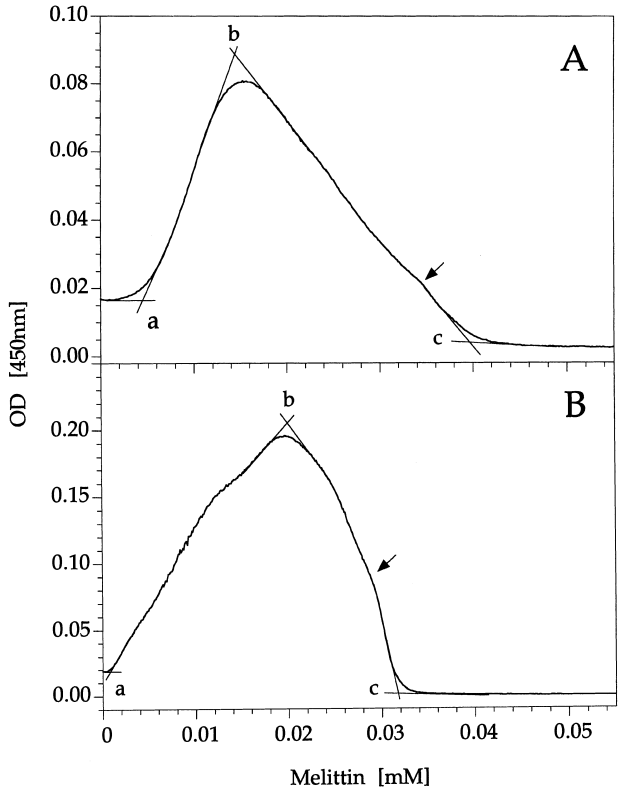

Fig. 4 A, B Representative variations of the optical density at 450 nm during continuous addition of melittin to SM (2) (**A**) and DPPC (**B**) small unilamellar vesicles at 37 °C. Initial lipid concentration was 0.4 mM. Break points (*a*, *b* and *c*) are indicated as determined by the intercept of the tangents to the curves. The *arrow* denotes a minor breakpoint (see text)

observed during continuous addition of melittin were not delayed owing to slow kinetics of the systems, different peptide injection rates were tested and found to have no detectable influence on the positions of the break points, although the absolute intensity at break point *b* was altered by modification of the injection rate. As a function of increasing (decreasing) phospholipid concentration the shapes of the OD curves remain the same, but the break points are shifted to higher (lower) melittin concentrations. This is evident from Fig. 5, where peptide concentrations at break points *a*, *b* and *c* are plotted as a function of phospholipid concentration. For all three break points the relation between the peptide and lipid concentration is a strictly linear one, demonstrating that the stoichiometry of the systems at a given breakpoint stays the same independent of the lipid concentration.

Discussion

Disc-to-vesicle transition of melittin-lipid complexes triggered by the gel-to-fluid phase transition

Interestingly, the SM/peptide system has the very same features as the DPPC/peptide system in both ^{31}P-NMR and

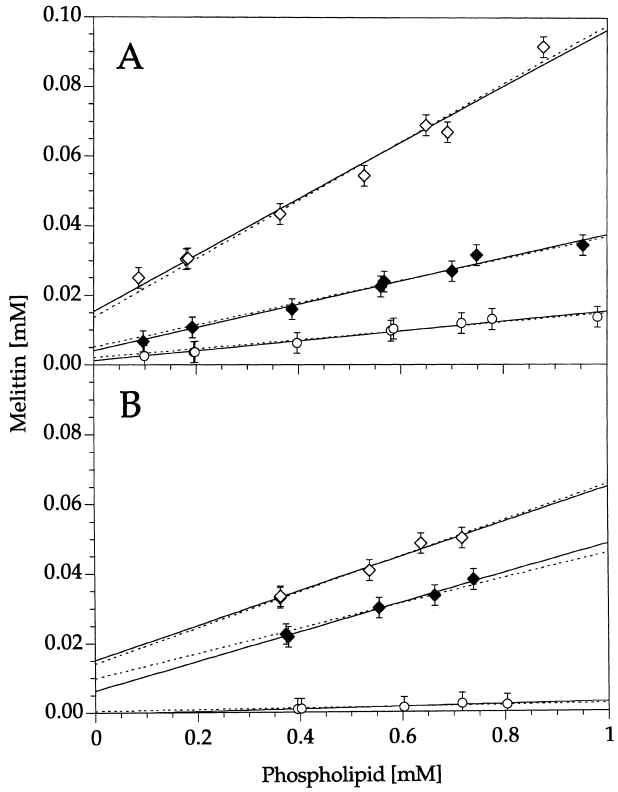

Fig. 5 A, B Melittin versus lipid concentration for SM (2) (**A**) and DPPC (**B**) at breakpoint *a* (○), *b* (◆) and *c* (◇) at 37 °C. The *solid lines* correspond to linear fits and the *dashed lines* were fitted with $K_p = 6.1 \pm 0.8$ mM^{-1} and 3.7 ± 0.4 mM^{-1} for SM (2) and DPPC vesicles (see text)

turbidity measurements (Figs. 1 A–C and Fig. 3 A). For $R_i > 5$ the system gives rise to broad and narrow isotropic ^{31}P-NMR lines in the lipid's fluid and gel phase, respectively, and a powder pattern for the gel-to-fluid phase transition region of the sphingolipid (Figs. 1 A–C and Table 1). Also, after incubation at 60 °C, the OD of the SM/melittin system at $R_i = 10$ stays approximately constant when the temperature is decreased until an important increase in the OD is observed when approaching T_m, followed by a clearing of the dispersion when the lipid's gel-phase is reached. This parallelism of turbidity and ^{31}P-NMR observations demonstrates that the thermotropic behavior of the system is due to strong changes in the size of the lipid/peptide complexes. Moreover, the similarity between the SM/mellitin system and the DPPC ones suggests, that the very same toxin-induced polymorphism is observed for SM as has been reported for PC/melittin systems (Dufourc et al. 1986 a; Dufourcq et al. 1986; Lafleur et al. 1987; Dufourc et al. 1989; Faucon et al. 1995). It is thus proposed that melittin induces the formation of small unilamellar vesicles (Dufourc et al. 1986 a; Dufourcq et al. 1986) in the fluid phase of natural SM, whereas in the gel phase small discoidal objects with the thickness of a single bilayer are formed (vesicle and disc diameter ≈4000 Å and ≈200 Å, respectively, for DPPC (Dufourc et al. 1986 a; Dufourcq et al. 1986)). The gel phase behavior of the SM/melittin system is particularly interesting because it shows that the toxin can trigger disc formation in the SM bilayer at physiological temperatures (vide supra).

Concerning the fusion or aggregation phenomenon at $\approx T_m$ of the lipid, the observation of an anisotropic ^{31}P-NMR powder pattern for the peptide containing SM and DPPC systems can be related to the formation of large objects having an average diameter ≥10 000 Å (Burnell et al. 1980). In the turbidity measurements this phenomenon is accompanied by a sharp increase in OD. As can be noted the temperature range in which this behavior is observed is larger in the NMR than in the turbidity measurements (compare Fig. 2 and Fig. 3 A). It is understandable that this is related to the different experimental conditions (continuous temperature variation vs. steady state, and lipid concentration of 1 vs. 60 mM) used in turbidity and NMR experiments. The disappearance of the disc-to-vesicle transition in the SM system when passing from $R_i = 10$ to $R_i = 5$ and the clear solution obtained independently of the physical state of the lipid further supports the analogy between SM and DPPC/toxin systems. For DPPC this lyotropic transition has been reported to be due to the formation of mixed micelles (Dufourc et al. 1986 a; Dufourcq et al. 1986). The same phenomenon is seemingly observed for bilayers composed of natural SM.

Differences between the melittin-containing SM and DPPC systems are only found in the amount of reorganized lipid (Fig. 2), which will be discussed in the following section, and in the thermal width of the fusion or aggregation process (see Fig. 3). Bovine brain SM, as a naturally occurring mixture of various sphingomyelin molecules, is rich in stearic (18 : 0) and nervonic acid (24 : 1) leading to a very broad gel-to-fluid phase transition in contrast to the well-defined transition of DPPC, which explains the difference in the thermal width of the fusion or aggregation process.

Process of disc formation at 37 °C

Melittin-induced disc formation occurs spontaneously, that is without incubation at high temperature, some degrees below T_m not only for DPPC (Monette et al. 1993; Pott and Dufourc 1995; Pott et al. 1996) but also for SM (2). However, this solubilization process during continuous addition of melittin is modulated when DPPC is replaced by SM (2) (Fig. 4). This difference can be quantified by calculation of the R_i^*, the lipid-to-Mel_{pl} molar ratio (Mel_{pl} is the amount of phospholipid-associated toxin), at break points *a*, *b* and *c* from the curves of the peptide versus phospholipid concentration (Fig. 5). The linear relationship between the toxin and the lipid concentration can be described by (Ollivon et al. 1988; Paternostre et al. 1988):

$$Mel_t = Mel_f + 1/R_i^* \times PL$$

where Mel_t corresponds to the total peptide concentration, Mel_f to the concentration of free peptide in the aqueous phase, and PL to the phospholipid concentration. The total lipid concentration and the amount of lipid in the

Table 2 Free melittin and effective melittin-to-phospholipid molar ratios at the break points *a*, *b* and *c* (T = 37 °C)

Break point	SM (2)		DPPC	
	Mel_f [μM]	$1/R_i^*$	Mel_f [μM]	$1/R_i^*$
a	1.2 ± 0.5 (2.1)	0.014 ± 0.001 (0.013)	–0.3 ± 0.5 (0.5)	0.003 ± 0.001 (0.002)
b	4.0 ± 0.9 (5.1)	0.033 ± 0.002 (0.032)	6.3 ± 1.2 (9.8)	0.042 ± 0.002 (0.036)
c	15.3 ± 2.4 (13.6)	0.081 ± 0.004 (0.084)	15.1 ± 2.1 (14.1)	0.050 ± 0.004 (0.052)

The values are reported are deduced from the linear fits in Fig. 5, values in parentheses were calculated with $K_p = 6.1 \pm 0.8$ mM^{-1} and 3.7 ± 0.4 mM^{-1} for SM (2) and DPPC, respectively (see text)

lipid/peptide complexes can be considered to be the same, owing to the very low solubility of the phospholipids. The results obtained for such linear curve fits are summarized in Table 2. From the slope of the curves in Fig. 5 R_i^*'s of approximately 71 and 333 were found for the onset of the increase in OD (break point a) for SM (2) and DPPC, respectively. In the case of solid state NMR experiments, where the samples are of high concentration, one may consider all peptide molecules to be associated with the lipids, i. e., $R_i^* \approx R_i$. In the case of gel-phase SM the presence of melittin results in an isotropic line at $R_i = 50$ but not at $R_i = 100$. These values surround the R_i^* of 71 for break point *a*. For gel-phase DPPC the isotropic line is already detected at $R_i = 100$, but also for a peptide content higher than that necessary to reach break point *a*. Hence, melittin incorporation into the bilayer up to break point *a* seems to occur in the absence of modifications in the macroscopic organization of the lipid. Consequently, the SM (2) bilayer can incorporate 4 to 5 fold more peptide than the DPPC membrane while remaining unaffected from a macroscopic point of view. One possible explanation lies in the lipid organization at 37 °C. At this temperature pure DPPC is in the $P_{\beta'}$-phase, whereas such a rippled phase has not been reported for bovine brain SM. Another argument might be that the greater stability of the SM bilayer is due to the fatty acyl chain composition of this natural lipid. Anyway, the increased stability of SM when compared to PC may play a role in the rather high stability of erythrocytes against melittin-induced hemolysis when compared to PC model membranes.

For the onset of the decrease in OD (breakpoint *b*) R_i^*'s were estimated to be about 30 for the sphingo- and 24 for the glycerolipid. In contrast to what has been reported for detergent-induced phospholipid solubilization (Paternostre et al. 1988) the onset of the melittin-triggered decrease in OD cannot be correlated with the first appearance of an isotropic line in the ^{31}P-NMR spectra ($R_i = 50$ and 100 for SM and DPPC, respectively). This apparent discrepancy becomes comprehensible with reference to the quasi elastic light scattering data of the DPPC/melittin system (Dufourcq et al. 1986). Therein the authors reported that for low peptide amount and $T < T_m$ the DPPC/melittin system becomes quite heterogeneous with coexistence of large objects and smaller ones with a hydrodynamic radius, R_H, from ≈430 Å to ≈2800 Å up to $R_i = 100$. Such objects would indeed result in the appearance of an isotropic line in the NMR spectra, although not corresponding to the discs (Dufourcq et al. 1986). The decrease in OD after break point *b* very probably corresponds to substantial disc formation, but it should be stressed that *b* is not necessarily the onset of disc formation.

Complete fragmentation of the SM (2) and DPPC bilayers is reached at $R_i^* \approx 12$ and ≈20, respectively. The R_i^* for DPPC/melittin complexes formed spontaneously at 37 °C is identical to the one obtained by Dufourcq and coworkers (20±2 (Dufourcq et al. 1986)). In contrast to our work, the discs in their study were obtained from pre-incubated samples, which is quite an important detail, as it confirms that the complexes formed spontaneously indeed correspond to the very same discoidal objects that originate from samples submitted to thermal treatment. The difference between the R_i^* in the SM (2) and the DPPC discs may be a consequence of the acyl chain composition of the sphingolipid. It has recently been reported that the stability of PC/melittin discs decreases with increasing length of the fatty acyl chains (Faucon et al. 1995). It might be proposed that the slight increase in bilayer thickness expected for bovine brain SM when compared to DPPC requires higher peptide amounts to cover the edges of the discs. On the other hand one may suggest that the SM discs are smaller than the DPPC discs, in order to accommodate the long chain SM molecules.

Estimation of the partition coefficient of melittin

In a very simple model and neglecting electrostatic repulsion one may define the partition coefficient, K_p, of melittin between vesicles and the aqueous medium by

$$K_p = (Mel_{pl}/PL)/Mel_f$$

Since $Mel_{pl}/PL = 1/R_i^*$, it follows that $K_p = 1/R_i^*/Mel_f$. In Fig. 6 $1/R_i^*$ values for major break points (*a*, *b* and *c*) are reported as a function of Mel_f. For better statistics minor breakpoints not reported in Fig. 5 (see for instance the "bump" indicated by an arrow in Fig. 4) were analyzed in the same way as the main breakpoints. They were found to show a linear dependency of Mel_t on PL and are also reported in Fig. 6. It can be recognized that the data points for both types of lipid are rather scattered and prohibit an accurate determination of K_p. Nevertheless, linear regressions of these data points lead to $K_p = 6.1 \pm 0.8$ mM^{-1} and 3.7 ± 0.4 mM^{-1} for SM (2) and DPPC at 37 °C as rough estimation. Insertion of these partition coefficients in the linear relationship between Mel_t and PL for break points *a*, *b* and *c* leads to reasonable fits (Fig. 5, dashed lines), indicating that the systems can be described by these K_p values. It is further noteworthy that values of K_p are of the same order of magnitude as K_p reported for the interaction of melittin with POPC vesicles (2.1 ± 0.2 mM^{-1} (Kuchinka and Seelig 1989)).

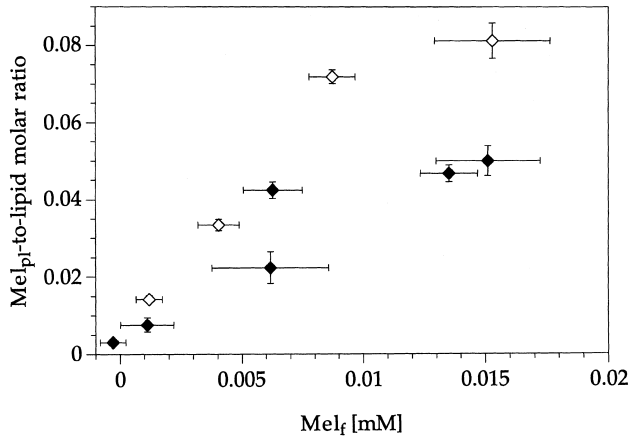

Fig. 6 Effective melittin-to-lipid molar ratio versus free melittin in the aqueous phase for major and minor break points for the SM (2) (◇) and the DPPC (◆) at 37 °C (see text for further details)

Conclusion

It has been shown herein that melittin induces a disc-to-vesicle transition triggered by the melting of the fatty acyl chains on the natural lipid sphingomyelin as in the case of the synthetic lipid DPPC. This is of interest in respect to the biological action of melittin. In the plasma membranes of mammals, such as erythrocytes, sphingomyelin is known to occur essentially in the outer leaflet where the peptide is first bound. The finding that the action of melittin on sphingomyelin is comparable to its effects on DPPC bilayers may establish the biological relevance of studies carried out with saturated phosphatidylcholines. In this context it should be mentioned that the peptide is able to induce disc formation, although to a lesser extent, in DPPC membranes containing a physiological cholesterol concentration (Pott and Dufourc 1995). The amount of such discoidal objects in the sterol-containing PC system was found to be maximum close to the T_m of the pure lipid. Because natural sphingomyelin has a gel-to-fluid transition temperature in the physiological temperature range and if disc formation occurs in a sterol-containing SM bilayer, such a lipid solubilization would be expected to occur around T_m and may be important in the understanding of the action of melittin on natural membranes. However, the implication of the melittin-induced polymorphism of SM systems for the peptide's action on biological systems (e. g., hemolysis) remains to be verified.

Acknowledgements We are grateful to Dr. J. Dufourcq for valuable discussions.

References

Barenholz Y, Thompson TE (1980) Sphingomyelins in bilayers and biological membranes. Biochim Biophys Acta 604: 129–158

Batenburg AM, Hibbeln JCL, Verkleij AJ, De Kruijff B (1987) Melittin induces H_{II} phase formation in cardiolipin model membranes. Biochim Biophys Acta 903: 142

Bello J, Bello HR, Granados E (1982) Conformation and aggregation of melittin: Dependence on pH and concentration. Biochemistry 21: 461–465

Bloom M, Davis JH, MacKay AL (1981) Direct determination of the oriented sample NMR spectrum from the powder spectrum for systems with local axial symmetry. Chem Phys Letters 80: 198–202

Boggs JM (1987) Lipid intermolecular hydrogen bonding: influence on structural organization and membrane function. Biochim Biophys Acta 906: 353–404

Brauner JW, Mendelsohn R, Prendergast FG (1987) Attenuated total reflectance fourier transform infrared studies of the interaction of melittin, two fragments of melittin, and δ-hemolysin with phosphatidylcholines. Biochemistry 26: 8151–8158

Brown LR, Braun W, Kumar A, Wüthrich K (1982) High resolution nuclear magnetic resonance studies of the conformation and orientation of melittin bound to a lipid-water interface. Biophys J 37: 319

Burnell EE, Cullis PR, de Kruijff B (1980) Effects of tumbling and lateral diffusion on phosphatidylcholine model membrane ^{31}P-NMR lineshapes. Biochim Biophys Acta 603: 63–69

Colotto A, Lohner K, Laggner P (1991) Small-angle X-ray diffraction studies on the effects of melittin on lipid bilayer assemblies. J Appl Cryst 24: 847–851

Compte M, Maulet Y, Cox J (1983) Biochem J 209: 269

Cornut I, Desbat B, Turlet JM, Dufourcq J (1996) In situ study by polarization modulated fourier transform infrared spectroscopy of the structure and orientation of lipids and amphipathic peptides at the air-water interface. Biophys J 70: 305–312

Curatolo W (1987) Biochim Biophys Acta 906: 111–136

Dempsey CE (1990) The action of melittin on membranes. Biochim Biophys Acta 1031: 143–161

Döbereiner H-G, Käs J, Noppl D, Sprenger I, Sackmann E (1993) Budding and fission of vesicles. Biophys J 65: 1396–1403

Dufourc EJ, Bonmatin JM, Dufourcq J (1989) Membrane structure and dynamics by ^{2}H- and ^{31}P-NMR. Effects of amphiphatic peptidic toxins on biological membranes. Biochimie 71: 117–123

Dufourc EJ, Faucon JF, Fourche G, Dufourcq J, Gulik-Krzywicki T, Le Maire M (1986 a) Reversible disc-to-vesicle transition of melittin-DPPC complexes triggered by the phospholipid acyl chain melting. FEBS Lett 201: 205–209

Dufourc EJ, Smith ICP, Dufourcq J (1986 b) Molecular details of melittin-induced lysis of phospholipid membranes as revealed by deuterium and phosphorus NMR. Biochemistry 25: 6448–6455

Dufourcq J, Faucon JF, Fourche G, Dasseux JL, Le Maire M, Gulik-Krzywicki T (1986) Morphological changes of phosphatidylcholine bilayers induced by melittin: vesicularization, fusion, discoidal particles. Biochim Biophys Acta 859: 33–48

Faucon JF, Bonmatin JM, Dufourcq J, Dufourc EJ (1995) Acyl chain length dependence in the stability of melittin-phosphatidylcholine complexes. A light scattering and ^{31}P-NMR study. Biochim Biophys Acta 1234: 235–243

Faucon JF, Dufourcq J, Lussan C (1979) The self-association of melittin and its binding to lipids – An intrinsic fluorescence polarization study. FEBS Lett 102: 187–190

Flach CR, Prendergast FG, Mendelsohn R (1996) Infrared reflection-absorption of melittin interaction with phospholipid monolayer at the air/water interface. Biophys J 70: 539–546

Frey S, Tamm LK (1991) Orientation of melittin in phospholipid bilayers. Biophys J 60: 922

Habermann E (1972) Bee and wasp venoms. Scinece 177: 314–322

Habermann E, Jentsch J (1967) Sequenzanalyse des Melittins aus seinen tryptischen und peptischen Spaltstücken. Hoppe-Seyler's Z Physiol Chem 348: 37–50

Hanke W, Methfessel C, Wilmsen HU, Katz E, GJ, Boheim G (1983) Melittin and a chemically modified trichotoxin form alamethicin-type multi-state pores. Biochim Biophys Acta 723: 108–114

Hermetter A, Lakowicz JR (1986) The aggregation state of melittin in lipid bilayers. An energy transfer study. J Biol Chem 261: 8243–8248

Hider RC, Khader F, Tatham AS (1983) Lytic activity of monomeric and oligomeric melittin. Biochim Biophys Acta 728: 206

Katsu T, Kuroko M, Morikawa T, Sanchika K, Fujita Y, Yamamura H, Uda M (1989) Mechanism of membrane damage induced by the peptides gramicidin S and melittin. Biochim Biophys Acta 983: 135 – 141

Kuchinka E, Seelig J (1989) Interaction of melittin with phosphatidylcholine membranes. Binding isotherm and lipid head-group conformation. Biochemistry 28: 4216 – 4221

Lad PL, Shier WT (1980) Arch Biochem Biophys 204: 418 – 424

Lafleur M, Dasseux JL, Pigeon M, Dufourcq J, Pezolet M (1987) Study of the effect of melittin on the thermotropism of dipalmitoylphosphatidylcholine by Raman spectroscopy. Biochemistry 26: 1173 – 1179

Lesieur S, Grabielle-Mandelmont C, Paternostre M-T, Moreau J-M, Handjani-Vila R-M, Ollivon M (1990) Action of octylglucoside on non-ionic monoalkyl amphiphile-cholesterol vesicles: study of the solubilization mechanism. Chem Phys Lipids 56: 109 – 121

Maulet Y, Brodbeck U, Fulpius B (1984) Selective solubilization by melittin of glycophorin A and acetylcholinesterase from human erythrocyte ghosts. Biochim Biophys Acta 778: 594 – 601

Mollay C, Kreil G (1974) Enhancement of bee-venom phospholipase A2 activity by melittin, direct-lytic factor and polymyxin B. FEBS Lett 46: 141 – 144

Monette M, van Calsteren MR, Lafleur M (1993) Effect of cholesterol on the polymorphism of dipalmitoylphosphatidylcholine/melittin complexes: An NMR study. Biochim Biophys Acta 1149: 319 – 328

Murata M, Nagayama K, Ohnishi S (1987) Membrane fusion activity of succinylated melittin is triggered by protonation of its carboxyl groups. Biochemistry 26: 4056

Nezil FA, Bayerl S, Bloom M (1992) Temperature-reversible eruption of vesicles in model membranes studied by NMR. Biophys J 61: 1413 – 1426

Ohki S, Marcus E, Sukumaran DK, Arnold K (1994) Interaction of melittin with lipid membranes. Biochim Biophys Acta 1194: 223 – 232

Ollivon M, Eidelman O, Blumenthal R, Walter A (1988) Micelle-vesicle transition of egg phosphatidylcholine and octyl glucoside. Biochemistry 27: 1695 – 1703

Olson FC, Munjal D, Malriya AN (1974) Structural and respiratory effects of melittin apis-mellifera on rat liver mitochondria. Toxicon 12: 419 – 425

Paternostre M-T, Roux M, Rigaud J-L (1988) Mechanisms of membrane protein insertion into liposomes during reconstruction procedures involving the use of Detergents. 1. Solubilization of large unilamellar liposomes (prepared by reverse-phase evaporation) by triton X-100, octyl glucoside, and sodium cholate. Biochemistry 27: 2668 – 2677

Podo F, Strom R, Crifo C, Zulauf M (1982) Dependence of melittin structure on its interaction with multivalent ions and lipid membranes. Int J Peptide Protein Res 19: 514 – 527

Pott T, Dufourc EJ (1995) Action of melittin on the DPPC-cholesterol liquid-ordered phase. A solid state ^{2}H and ^{31}P-NMR study. Biophys J 68: 965 – 977

Pott T, Dufourcq J, Dufourc EJ (1996) Fluid or gel phase lipid bilayers to study peptide-membrane interactions? Eur Biophys J 25: 55 – 59

Rance M, Byrd RA (1983) Obtaining high-fidelity spin 1/2 powder spectra in anisotropic media: phase-cycled Hahn echo spectroscopy. J Magn Res 52: 221 – 240

Seelig J, Seelig A (1980) Lipid conformation in model membranes and biological membranes. Quart Rev Biophys 13: 19 – 61

Sessa G, Freer JH, Colacicco G, Weismann G (1969) Interaction of a lytic polypeptide melittin with lipid membrane systems. J Biol Chem 244: 3575 – 3582

Shipley GG, Avecilla LS, Smal DM (1974) Phase behavior and structure of aqueous dispersions of sphingomyelin. J Lipid Res 15: 124 – 131

Smith R, Separovic F, Milne TJ, Whittaker A, Bennett FM, Cornell BA, Makriyannis A (1994) Structure and orientation of the pore-forming peptide, melittin, in lipid bilayers. J Mol Biol 241: 456 – 466

Sternin E, Bloom M, MacKay AL (1983) De-Pake-ing of NMR Spectra. J Magn Res 55: 274 – 282

Talbot JC, Dufourcq J, De Bony J, Faucon JF, Lussan C (1979) Conformational change and self-association of monomeric melittin. FEBS Lett 102: 191 – 193

Tosteson MT, Tosteson DC (1984) Activation and inactivation of melittin channels. Biophys J 45: 112 – 114

Weaver AJ, Kemple MD, Brauner JW, Mendelsohn R, Prendergast FG (1992) Fluorescence, CD, Attenuated total reflectance (ATR) FTIR and ^{13}C NMR characterization of the structure and dynamics of synthetic melittin and melittin analogues in lipid environments. Biochemistry 31: 1301 – 1313